Proceedings of the 41st IEEE
Conference on Decision and Control
Las Vegas, Nevada USA, December 2002

A Novel Electrocardiogram Segmentation Algorithm Using a Multiple Model Adaptive Estimator

Gregory S. Hoffman, Air Force Institute of Technology
Mikel M. Miller, Air Force Institute of Technology
Matthew Kabrisky, Air Force Institute of Technology
Peter S. Maybeck, Air Force Institute of Technology
John F. Raquet, Air Force Institute of Technology

Abstract

This paper presents a novel electrocardiogram (ECG) processing algorithm design based on a Multiple Model Adaptive Estimator (MMAE) for a physiological monitoring system. Twenty ECG signals from the MIT ECG database were used to develop system models for the MMAE. The P-wave, QRS complex, and T-wave segments from the characteristic ECG waveform were used to develop hypothesis filter banks. The MMAE robustly locates these key temporal landmarks in the ECG signal, extracting crucial patient treatment information from the often distorted or unstable ECG waveform. By adding a threshold filter-switching algorithm to the conventional MMAE implementation, the device mimics the way a human analyzer searches the complex ECG signal for a useable temporal landmark and then branches out to find the other key wave components and their timing.

Using a conditional hypothesis-testing algorithm, the MMAE correctly identified the ECG signal segments corresponding to the hypothesis models with a 96.8% accuracy-rate for the 11539 possible segments tested. The robust MMAE algorithm also detected any misalignments in the filter hypotheses and automatically restarted filters within the MMAE to synchronize the hypotheses with the incoming signal. Finally, the MMAE selects the optimal filter bank based on incoming ECG measurements. The algorithm also provides critical heart-related information such as heart rate, QT, and PR intervals from the ECG signal.

Introduction

This paper details the software algorithms required to extract information from an electrocardiogram (ECG), which may relate an event or a relationship between events in the ECG to the possibility of a dangerous physical condition. The heart's electrical activity not only contains information about how quickly the cardiac muscle is contracting and relaxing, but also contains information regarding the balance between the sympathetic nervous system (SNS) and parasympathetic nervous system (PNS). The SNS generally increases heart rate, and the PNS decreases heart rate. Other relationships between the events in the ECG may be found during strenuous situations, including fires, law enforcement situations, combat, or injury.

The research studied sample ECG signals and analyzed possible segmentation techniques. Hypothesized system models were developed based on the insight gained from sample ECG signal analysis. The hypothesized models were used in the ECG segmentation algorithm and the performance was tested on sample signals.

Electrocardiogram

An electrocardiogram (ECG) measures the heart's electrical activity. The ECG signal shows the voltage in the heart muscle as it contracts and relaxes, as measured from a spot on the body (different positions for the ECG leads will show different voltage levels). Figure 1 shows an ECG signal and the signal components. In a normal, healthy human, the signal starts at the sinoatrial (SA) node at the top of the heart, triggering the atria, which contract and relax (P-wave). The signal slows significantly at the atrioventricular (AV) node, allowing the ventricles to fill. The signal travels down the right and left bundle branch triggering the ventricle which then contracts (QRS) and relaxes (T), (U). The heart is then relaxed until the next "heart beat," starting with the P- wave. Figure 1 shows the characteristic waveform with the corresponding heart activity. The shaded areas in the diagram represent the electrical signal traveling through the heart.

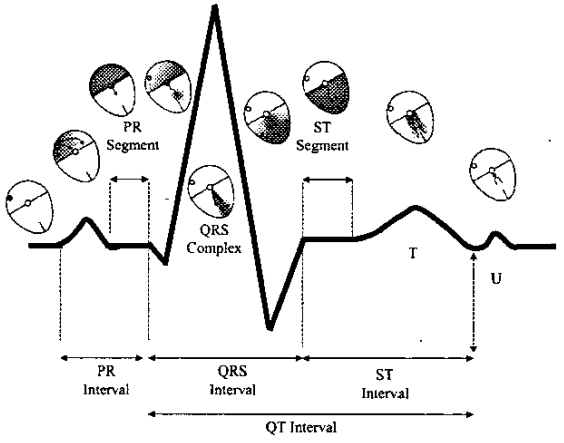

Figure 1. ECG Characteristic Waveform Corresponding to Heart Activity [1]

The ECG waveform should follow the standard "P, Q, R, S, T, U" distinct electrical events in the heart [2]. The signal obtained during an ECG recording depends on several facts: (1) the location of the leads, (2) how well the leads are placed on the skin, (3) the quality of the signal amplifiers, and (4) the amount of measurement noise.

The relationships between segments of the ECG signal provide significant information as to what events and activities occur in the body [4, 5]. This research proposes the use of a multiple model adaptive estimator (MMAE) to identify the ECG segments. A multiple model filter bank has been used extensively in guidance, navigation, and control applications to detect parameter changes in the system [6]. Willsky reported great success in arrhythmia detection and classification in electrocardiograms using both a multiple hypothesis model and the generalized likelihood ratio (GLR) [7, 8]. These systems, however, already had the different ECG segments decomposed from the ECG signal; they merely analyzed and identified changes in the relationships among the segments. This research,

however, uses the MMAE as the basis for the ECG segmentation algorithm.

MMAE

When a system has certain characteristics or parameters that can change, the system model used in the filtering algorithm may be invalid. The Kalman filter performance is only as good as the models used in the algorithm. Any characteristics not included in the model make the Kalman filter a suboptimal estimator. One way to deal with the uncertainties in the model is to develop a multiple model, filtering algorithm. A multiple model adaptive estimator (MMAE) is a bank of parallel Kalman filters, each with a different filter model and an algorithm to test for the adequacy of the assumed model in each filter [9]. One could create a discretized parameter space from the continuous parameter space of all possible parameter values. Let **a** be a vector of all possible parameter values $\{\mathbf{a}_1, \mathbf{a}_2,\ldots,\mathbf{a}_J\}$ $(j=1,2,\ldots J)$. The parameter vector in this problem is the different system models for the QRS complex, T-wave, and P-wave.

A block diagram of the MMAE is shown in Figure 2. Note the outputs of the hypothesized system models are scaled by a probability weighting computation.

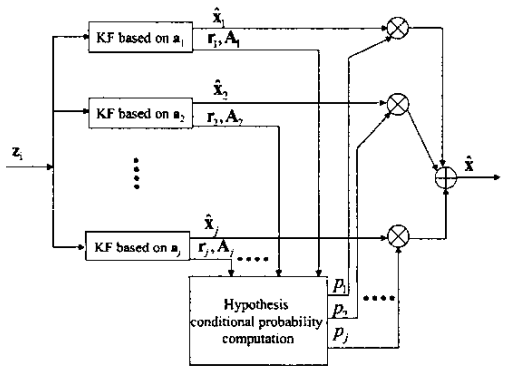

Figure 2. Multiple Model Filtering Algorithm Block Diagram

The hypothesis conditional probability computation in Figure 2 is a conditional probability that the parameter vector **a** assumes the true value $\mathbf{a}_j$ conditioned on the measurement history $\mathbf{Z}_i$, defined as

$$p_j(t_i) = prob\{\mathbf{a} = \mathbf{a}_j \mid \mathbf{Z}(t_i) = \mathbf{Z}_i\}. \quad (1)$$

The probability of each filter modeling the true system can be evaluated as a function of both the vector of parameter values and the measurement history through a probability density function and the probability weighting at a sample time earlier:

$$p_j(t_i) = \frac{f_{\mathbf{z}(t_i)\mathbf{a},\mathbf{Z}(t_{i-1})}(\mathbf{z}_i \mid \mathbf{a}_j, \mathbf{Z}_{i-1}) p_j(t_{i-1})}{\sum_{n=1}^{J} f_{\mathbf{z}(t_i)\mathbf{a},\mathbf{Z}(t_{i-1})}(\mathbf{z}_i \mid \mathbf{a}_n, \mathbf{Z}_{i-1}) p_n(t_{i-1})} \quad (2)$$

The conditional density function of the current measurement vector $\mathbf{z}(t_i)$ based on the parameter vector $\mathbf{a}_j$ and the measurement history $\mathbf{Z}_{i-1}$ can be shown to be [9]:

$$f_{\mathbf{z}(t_i)\mathbf{a},\mathbf{Z}(t_{i-1})}(\mathbf{z}_i \mid \mathbf{a}_j, \mathbf{Z}_{i-1}) = \frac{1}{(2\pi)^{m/2}\left|\mathbf{A}(t_i)\right|^{1/2}} \exp\{L_j(t_i)\} \quad (3)$$

where

$$L_j(t_i) = -\frac{1}{2}\mathbf{r}_j^T(t_i)\mathbf{A}_j(t_i)^{-1}\mathbf{r}_j(t_i)$$

and m is the number of measurements. When filter j's model matches the true system, the residual vector $\mathbf{r}_j(t_i)$ will be zero mean with covariance $\mathbf{A}_j(t_i)$. Filter probabilities are started out such that $p_j(t_i)=1/J$ and are then updated after each measurement incorporation by Equation (3). Note that the denominator is a scaling factor to ensure that the filter probabilities add up to one. In certain cases, the elemental filter residuals can seem good causing the filter to generate an erroneous probability, especially if its residual is going through zero at the time of the update.

System Modeling

Based on the visual waveform segmentation, a segment power spectral density estimate was formed for each segment type. The ECG segments were found to be well modeled by a stochastic process whose output power spectral density was a bandpass filter [10]. A bandpass filter's transfer function can be described as:

$$G(s) = \frac{s + w_n}{s^2 + 2\alpha s + w_n^2} \quad (4)$$

where α is the half power frequency from the center frequency, ω_c, and ω_n is $(\alpha^2+\omega_c^2)^{0.5}$. This filter always gives a peak value of $\sigma^2\alpha$ (where σ^2 is the gain) with the assumption that the driving function is white Gaussian noise (WGN) and has strength $2\alpha\sigma^2$. This bandpass filter form allows easy center frequency and bandpass region width manipulation. The Kalman filter model is then:

$$\underbrace{\begin{bmatrix}\dot{x}_1(t)\\ \dot{x}_2(t)\\ \dot{x}_3(t)\end{bmatrix}}_{\dot{\mathbf{x}}(t)} = \underbrace{\begin{bmatrix}0 & 1 & 0\\ 0 & 0 & 1\\ 0 & -\omega_n^2 & -2\alpha\end{bmatrix}}_{\mathbf{F}} \underbrace{\begin{bmatrix}x_1(t)\\ x_2(t)\\ x_3(t)\end{bmatrix}}_{\mathbf{x}(t)} + \underbrace{\begin{bmatrix}0\\ 1\\ \omega_n - 2\alpha\end{bmatrix}}_{\mathbf{G}} w(t) \quad (5)$$

The input scalar, zero mean, WGN driving term has statistics:

$$E\{w(t)w(t+\tau)\} = Q(t)\delta(\tau) = 2\alpha\sigma^2\delta(\tau) \quad (6)$$

These statistics come from the transfer function's assumption that the input WGN strength is $2\alpha\sigma^2$. Measurements were available discretely as a function of the states and additive WGN:

$$z(t_i) = \begin{bmatrix}1 & 0 & 0\end{bmatrix}\mathbf{x}(t_i) + v(t_i) \quad (7)$$

The zero mean v statistics were as follows:

$$E\{v(t_i)v(t_j)^T\} = \begin{cases} R(t_i) & t_i = t_j \\ 0 & t_i \neq t_j \end{cases} \quad (8)$$

In this research, a different approach than the Bayesian method used by the MMAE blending is used to determine the correct hypothesis. The *maximum a posteriori* (MAP) MMAE design uses the elemental filter containing the highest probability hypothesis rather than the Bayesian blending as in Figure 2. Because the assumption was made that ECG segment cannot be a combination of hypotheses for distinguishability purposes, the highest probability filter does make logical sense in this application.

Online Hypothesis Swapping Algorithm

Because the ECG signal is "pseudo-periodic," more information is known about the signal than the algorithm is initially "telling" the MMAE. For example, it is assumed that the T-wave typically follows the QRS complex. Following the T-

wave is a "rest" period, and following the "rest" period is the P-wave. The filter takes advantage of this segment order information to help it determine when the specific segment starts and ends. Therefore, the MMAE doesn't need to calculate which of the four hypotheses is correct. Therefore, this event order information narrows down which of the MMAE hypotheses are correct. Once the algorithm is locked onto the QRS complex, it no longer has to distinguish between the similar T and P-waves. The algorithm is initialized to choose between two online filters, one tuned for the QRS complex and another tuned for lower frequency and lower strength signals. The hypothesis filter parameters for the initialization bank are shown in Table 1.

Table 1. Initialization Hypothesis Filter Bank Parameters

Hypothesis	Not QRS	QRS Complex
ω_c	25	100
σ^2	50	30000
α	2	2

An offline filter bank containing hypotheses for the characteristic ECG waveform is also initialized. The online filter bank waits until the QRS complex hypothesis in filter two is detected for at least five consecutive samples. This eliminates much of the possible jitter in the probability calculation and ensures that the QRS complex hypothesis is consistent for an extended time. Once the QRS complex is declared, the correct hypothesis, the first online elemental filter's state transition matrix, Φ, and equivalent discrete-time noise, $\mathbf{Q}_d$, are replaced with the Φ and $\mathbf{Q}_d$ from the offline T-wave hypothesis. When the new hypothesis is brought online, the conditional hypothesis probabilities are reset to the lower bounds for the online T-wave and the QRS complex hypotheses that were just declared correct. The online filters continue with the normal MMAE propagate and update cycle. These two filters remain online until the T-wave filter is declared correct for five samples in the same manner as the QRS complex was declared correct. This process continues, with the two hypotheses in the online filter bank at any one time being the correct hypothesis and the next expected corrected hypothesis. Thus, the hypothesis-testing algorithm never has to distinguish between four hypotheses, only two.

The filter swapping routine can get unsynchronized with the ECG signal due to irregularities in the waveform or filter swap incorrect timing. If the filter bank is not synchronized, the QRS hypothesis will not be online at the correct time. When the QRS complex measurements are used in the MMAE, high residuals in the two online hypothesis filters will result in a high likelihood quotient, L, from Equation (3).

If the hypothesis model matches the true system model, the likelihood quotient and the number of measurements will be approximately equal. Thus, if the QRS hypothesis is not online at the correct time, the filter bank can be declared out of sync if a likelihood quotient is detected above a threshold. The threshold value of 10 gives a safety margin to account for signal changes during the ECG recording, while ensuring that when the filter bank is not synchronized, a restart is declared as quickly as possible. When the restart is declared, the filter banks are reinitialized to the starting values and the swapping routine waits for the next QRS complex declaration to begin.

A correct hypothesis declaration by the MMAE effectively provides a sample segment over which the hypothesis best matches the data. This correct hypothesis restricts the sample region that an algorithm has to search over to find a specific segment area of interest. The RR, QT, and PR intervals are easily calculated using the P, R, and T-wave peaks and the correct QRS complex hypothesis start for the Q-wave.

The animal exsanguination data from Qualia Computing, Inc. [11] provided a special challenge not seen in the MIT ECG data files [12]. The heart rate increased as time went on, the signal waveforms change shape, the T-wave changed location, and the signal strength decreased dramatically. Two additional MMAE filter banks were created and the ability to switch to a new bank was created. The new filter banks were very similar to the original filter banks with the only changes residing in tuning the filter bank to a particular signal section. Lower input WGN strengths for each hypothesis and a switch to the new filter banks at the proper time allowed the MMAE ECG processing algorithm to continue functioning properly. Table 2 through Table 4 show the tuning parameters for the ECG segment hypotheses and the lowering Q values in the alternate filter banks.

Table 2. Hypothesis Filter Bank Parameters

Hypothesis	QRS Complex	T-wave	Rest	P-wave
ω_c	100	100,10,100	10	100
σ^2	30000	50, 0.50, 50	0.5	30
α	2	2	2	2

Table 3. Alternative Hypothesis Filter Bank Parameters, Bank 2

Hypothesis	QRS Complex	T-wave	Rest	P-wave
ω_c	100	100,10,100	10	100
σ^2	15000	20, 0.70, 20	0.7	15
α	2	2	2	2

Table 4. Alternative Hypothesis Filter Bank Parameters, Bank 3

Hypothesis	QRS Complex	T-wave	Rest	P-wave
ω_c	100	100,10,100	10	100
σ^2	5000	5, 1, 5	0.7	10
α	2	2	2	2

The QRS complex hypothesis WGN input was tuned such that the likelihood quotient, $L_j(t_i)$, was approximately four. Again, this is tighter tuning than would normally be performed, remembering that $L_j(t_i)$ is approximately the number of measurements with conservative tuning. The other filter hypotheses' WGN values were also reduced based on the hypothesis calculation transitions.

The additional offline filter banks allow for an increase in the algorithm's robustness because an algorithm can be created to take advantage of both the restart routine and the offline filter bank switch routine. If a signal has characteristics that do not fit the first online filter bank, the algorithm will restart several times. The filter bank starts with bank one and uses the restart algorithm to determine when to try the next filter bank. If the difference between the number of restarts and the detected R-waves is two or three, the next filter bank is used in the swapping routine. Thus, if the signal does not initially match the hypotheses in filter bank one, several restarts will occur. The MMAE was given a chance to synchronize the filter banks with the signal. When three restarts happen in a row, filter bank one was switched to filter bank two. All variables were reinitialized, including the number of restarts and the number of R-waves detected.

Overall MMAE ECG Processing Algorithm Description

The overall MMAE ECG processing algorithm is depicted in the flow diagram shown in Figure 3. Following the path through the diagram, first the MMAE is initialized as outlined in the initialization and restart routine. Once the filter banks are

synchronized with the signal, the MMAE begins the overall propagate and update routine. Every sample is checked by the restart routine to ensure that the online filters are synchronized with the signal.

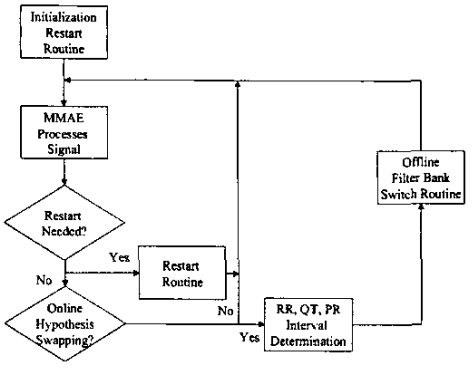

Figure 3. MMAE ECG Processing Flow Chart with Subroutines

If a restart is needed, the restart routine is followed. Next, the hypothesis swapping routine checks if the online filter hypotheses need to be swapped with offline hypotheses. If a swap is needed, the interval calculation routine is run; if not, the algorithm continues processing data. After the intervals are calculated, the offline filter bank switching routine is used to check if offline filter banks can better match the signal measurements. The algorithm continues processing ECG data until the signal end.

Results

The MMAE ECG processing algorithm was used to analyze 20 ECG signals obtained from the MIT ECG database used in the system model development. The algorithm's ability to detect the R-waves accurately and to determine the heart rate was first analyzed. The R-wave detection accuracy was defined as follows:

$$Accuracy = \frac{\text{R-wave}}{\text{R-wave + Restart}} \qquad (9)$$

where R-wave is the number of R-waves detected correctly and Restart is number of restarts during the processing. The accuracy measured how well the algorithm determined the QRS complex location. It was penalized for restarts and was penalized for missed R-waves. It was found that even though the MMAE algorithm restarted when required, it never incorrectly identified an R-wave and failed to restart. Thus, the R-wave count contains only true R-wave peaks, not T-wave or P-wave peaks that may be identified before a restart. Therefore, the heart rate plot contains no intervals where the R-wave peak may have been incorrectly identified.

The algorithm hinged on correctly finding the QRS complex, restarting the algorithm if it did not, and calculating the QT and the PR intervals when possible. The algorithm scoring is shown in Table 5. This accuracy score was very important to the algorithm's performance analysis. Clearly, the algorithm scored well when the ECG lead placement measured all events in the characteristic ECG waveform. Table 5 clearly shows the measurement lead effect on the MMAE algorithm's performance. In the following sections, three sample signals will be analyzed. ECG 3 was from modified Lead III and Lead V4 (a chest lead rather than a limb lead). This sample clearly shows the MMAE algorithm's good and bad performance throughout the ECG sample.

Table 5. MMAE ECG Processing Algorithm Scoring

Sample	Signal	R-Wave Detected	Restarts	Accuracy	Lead
ECG 3	1	55	2	96.49%	V4
	2	16	29	35.56%	MLIII
ECG 5	1	52	0	100.00%	V4
	2	19	17	52.78%	MLIII
ECG 11	1	53	35	60.23%	MLIII
	2	56	1	98.25%	V4
ECG 13	1	9	40	18.37%	MLIII
	2	60	0	100.00%	V4
ECG 19	1	57	0	100.00%	V4
	2	56	8	87.50%	MIII
ECG 21	1	72	0	100.00%	V4
	2	66	6	91.67%	MLIII
ECG 23	1	70	4	94.59%	V4
	2	70	4	94.59%	MLIII
ECG 25	1	68	0	100.00%	V4
	2	67	0	100.00%	MLIII
ECG 27	1	69	0	100.00%	V4
	2	66	0	100.00%	MLIII
ECG 39	1	66	29	69.47%	MLIII
	2	74	3	96.10%	V4

Signal 1 from lead V4 followed the characteristic ECG waveform as expected by the MMAE. The processed results are shown in Figure 4 and Figure 5. Figure 4 shows the ECG signal with the MAP hypothesis overlaid. The hypotheses are strictly a one or two, corresponding to the online hypothesis filter number. Note that the hypotheses were correctly brought online according to the swapping method.

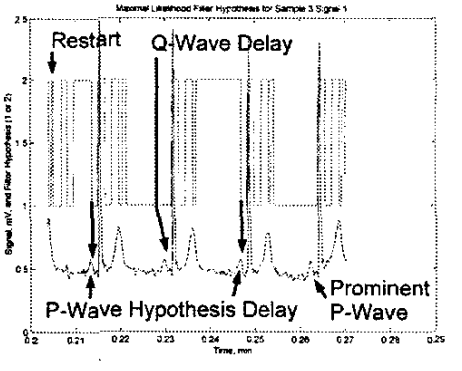

Figure 4. Maximal Likelihood Filter Hypothesis for Sample 3 Signal 1

The hypothesis swapping, as demonstrated Figure 4, worked well except for the cases noted where the P-wave hypothesis was declared correct after the peak of the P-wave. The restart algorithm's performance worked well, as shown by the restart declared at 0.204 minutes and the algorithm accurately locked onto the next QRS complex. The restart was declared because the low frequency filter did not match the positive slope to negative slope change well and the scalar likelihood quotient went above the pre-specified restart value of 10. While a higher restart value would have allowed the MMAE to continue with the hypothesis swapping without the restart, the filter bank synchronized itself perfectly with the next QRS complex.

The R-wave was consistently identified, yielding a well-formed heart rate plot as shown in Figure 5. Note that the region between 0.15 to 0.20 minutes is caused by the two restarts. The

ECG Sample 3 Signal 2 characteristics were very different from those of Signal 1, as shown in Figure 6. The modified Lead III signal had no QRS complex from the characteristic waveform.

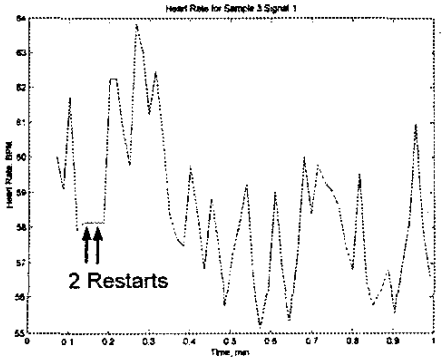

Figure 5. ECG Sample 3 Signal 1 Heart Rate

The R-wave was not present, slowing the center frequency of the QRS complex down because there was one fewer wave. The P-wave was buried in the noise during the rest section causing severe problems for the hypothesis-swapping algorithm. Consequently, the accuracy score for signal 2 was the second lowest compared to all other accuracy scores. The reason for the problems with the MMAE algorithm was very simple: the hypothesis banks did not model the signal well. Note the restart at 0.23 minutes and the poor hypothesis swapping performance in Figure 6.

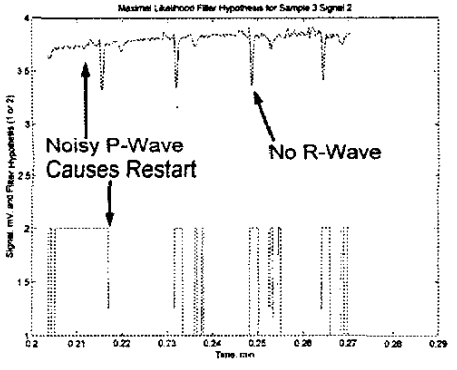

Figure 6. Maximal Likelihood Filter Hypothesis for Sample 3 Signal 2

The ECG 3 signal 2 shown in Figure 6 reveals conditions in the signal that the algorithm cannot handle. However, the algorithm could be improved by developing a hypothesis that recognizes when the P-wave is buried in noise, allowing the MMAE to continue processing the signal correctly.

The animal exsanguination ECG data was especially difficult to process due to the changing heart rate, changing waveform, and changing signal to noise ratio. Although the accuracy scores drop during segments of the signal, the heart rate was still determined very well. As shown in Figure 7, until the 86-minute mark in the data set, the heart rate was tightly packed, except every 20 minutes from the 16-minute mark onwards. The results are shown in Figure 7 and Figure 8.

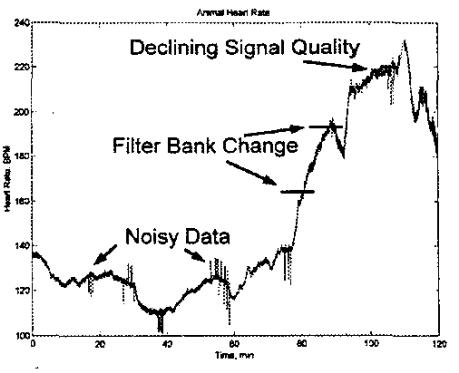

Figure 7. Animal Heart Rate During Exsanguination

Note the seamless transition between filter bank models at 165 BPM and again at 195 BPM, which were brought online by simply changing the bank used to select the two online hypotheses.

The PR interval was also noisy in several signal segments, as shown in Figure 8.

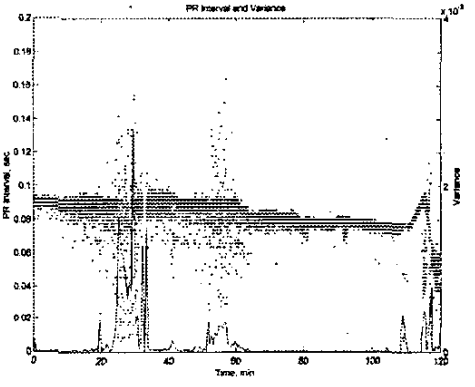

Figure 8. Animal Exsanguination PR Interval and PR Interval Variance

Figure 8 also shows the PR interval variance which is related to the RR interval variance and shows the balance between the PNS and the SNS as previously mentioned. Note that the variance initially increases dramatically and then decreases. This is the first known correlation of beat-to-beat variation with severe blood loss. However, in sections where the signal was noisy and the R-wave determination was difficult, the P-wave determination was even more difficult. A correct QRS complex hypothesis did not guarantee the P-wave peak accuracy due to the other spikes or peaks in the signal.

Conclusions

The MMAE ECG processing algorithm developed in this research performed extremely well when the signal of interest contained the ECG characteristic waveform components. It was shown that the electrode lead placements measured different heart events and very clearly affected the MMAE algorithm's performance. In 12 out of the 38 signals, 32 minutes of data, the ECG processing algorithm did not have a restart and perfectly found the heart rate. Moreover, in 26 out of the 38 signals, the

algorithm had an accuracy score over 0.90. The overall MMAE ECG processing algorithm accuracy is shown in Table 6.

Table 6. Overall Algorithm Accuracy

Data Set	R-wave	Restart	Accuracy
MIT-best	633	10	98.44%
Animal-best	10542	354	96.75%
Total-best	11175	364	96.85%

When the data set is reduced to include signals from just lead V4, the accuracy is 98.4%. The MMAE algorithm processed the animal ECG data with 87.5% accuracy for the whole data set. Because the signal strength during the last three signal segments is very low, these last segments can be removed to form a data set that generally fits the MMAE models. The accuracy score for the combined first 15 data sets was 94.7%. Finally, three noisy data segments where the T-wave or P-wave was indistinguishable from other extraneous signal peaks can also be removed. The accuracy score for these "best" fit signal segments was 96.8%.

Finally, the combined total scores are also shown in Table 6. If the data sets are restricted to those containing the characteristic ECG waveform as the algorithm expects, the accuracy jumps to 94.8%. In addition, if the animal exsanguination signals that were very noisy were taken out, the accuracy would jump to 96.8%. When the algorithm correctly found the QRS complex, it subsequently could find the T-wave peak and the P-wave peak with high probability.

The algorithm's weaknesses were also identified by the signals that it could not process with high accuracy. The 12 signals where the algorithm did not perform well represent signals where the algorithm could not identify the T-waves or P-waves in the signal due to excess noise or the lead placement choice. However, it is important to note that the hypothesis models were not developed based on these types of signals. It was pointed out that additional models could easily be developed and integrated into the MMAE filter banks to make the MMAE ECG processing algorithm more robust.

The solutions to the current algorithm's shortcomings are being developed. The hypothesis-swapping algorithm is very similar to a hidden Markov model. The MMAE can readily incorporate transition probabilities, clearly indicating the expected transition order such as QRS complex to T-wave, T-wave to rest, and rest to P-wave. Thus, the probability flow is controlled by the transition probabilities rather than the hypothesis-swapping algorithm. Additionally, the MMAE can be implemented in a hierarchical structure when more. This technique can be applied to the ECG segmentation algorithm to make the hypothesis swapping a parallel implementation as opposed to this algorithm's sequential nature. Finally, when the MMAE filter banks can be switched in and out automatically, additional banks can be created with hypothesized arrhythmias. This bank can run in parallel to the other banks, looking just for the arrhythmias.

Using this unique technique, it has been exhibited for the first time, the temporal sequence of beat-to-beat time variation during severe blood loss over a period of several hours. Such data should make possible the early detection of the cascade of events that leads to fatal irreversible shock in severe injury accidents. Such shock is the cause of death in 40% of civilian accident injury and 66% of wartime injury. This analyzer could be easily added as a software update to the standard physiological monitors universally used in emergency vehicles and treatment facilities.

Disclaimer

The views expressed in this paper are those of the authors and do not reflect the official policy or position of the United States Air Force, Department of Defense, or the U.S. Government.

References

[1] Klimes, R. "EKG Review: Characteristics and Interventions." Excerpt from online course. n. pag. http://www.ce5.com/ekg100.htm. 14 Sep 01.

[2] Stern, Robert M., William J. Ray, Karen S. Quigley. *Psychophysiological Recording.* Oxford: University Press, 2001.

[3] Brennan, M., M. Palaniswami, and P.W. Kamen. "A New Cardiac Nervous System Model for Heart Rate Variability Analysis," *Proceedings of the 20th Annual International Conference of the IEEE Engineering in Medicine and Biology Society.* 349-352. New York: IEEE Press, 1998.

[4] Fujisawa, Hiroyuki, Rakashi Uozumi, and Koichi Ono. "Evaluation of Autonomic Nervous System with Correlation Diagram of R-R Interval and P-R Interval," *Proceedings of the 20th Annual International Conference of the IEEE Engineering in Medicine and Biology Society.* 353-356. New York: IEEE Press, 1998.

[5] Botzer, L., B. Strasberg, and S. Abboud. "Dynamic QT-RR Relationships in 12 lead ECG in Patients with Coronary Artery Disease," *Computer in Cardiology*, 27:163-166 (2000).

[6] Willsky, Alan S. "A Survey of Design Methods for Failure Detection in Dynamic Systems." *Automatic,* 12: 601:611 (1976).

[7] Gustafson, A.S., Willsky, and J.Y. Wang. "Final Report: Cardiac Arrhythmia Detection and Classification Through Signal Analysis." The Charles Stark Draper Laboratory, Cambridge, MS,. Report R-920 (July 1975).

[8] Zyweitz, Christian and B. Schneider. "Computer Application on ECG and VCG Analysis, North Holland, 1973.

[9] Maybeck, Peter S. *Stochastic Models, Estimation and Control, II.* New York: Academic Press, Inc. 1982. Republished Arlington VA: Navtech, 1994.

[10] Hoffman, Gregory S. A Novel Electrocardiogram Segmentation Algorithm Using a Multiple Model Adaptive Estimator. MS Thesis. AFIT/GE/ENG/02M-10, School of Engineering, Air Force Institute of Technology (AU), Wright-Patterson AFB OH, March 2002.

[11] Amburn, Phillip. Qualia Computing, Inc. Beavercreek, OH. Personal Interview. 29 Jan 02.

[12] Goldberger AL, Amaral LAN, Glass L, Hausdorff JM, Ivanov PCh, Mark RG, Mietus JE, Moody GB, Peng CK, Stanley HE. PhysioBank, PhysioToolkit, and Physionet: Components of a New Research Resource for Complex Physiologic Signals. *Circulation* 101(23):e215-e220 [Circulation Electronic Pages; <http://circ.ahajournals.org/cgi/content/full/101/23/e215>]; 2000 (June 13).